

# Microwave Fields Have Little Effect on $\alpha$ -Synuclein Aggregation in a *Caenorhabditis elegans* Model of Parkinson's Disease

David I. de Pomerai,<sup>1\*</sup> Nooria Iqbal,<sup>1</sup> Ivan Lafayette,<sup>1</sup> Archana Nagarajan,<sup>1</sup> Mehri Kaviani Moghadam,<sup>1</sup> April Fineberg,<sup>1</sup> Tom Reader,<sup>1</sup> Steve Greedy,<sup>2</sup> Chris Smartt,<sup>2</sup> and David W.P. Thomas<sup>2</sup>

<sup>1</sup>School of Biology, University of Nottingham, Nottingham, United Kingdom

<sup>2</sup>Department of Electrical and Electronic Engineering, University of Nottingham, Nottingham, United Kingdom

Potential health effects of radiofrequency (RF) radiation from mobile phones arouse widespread public concern. RF fields from handheld devices near the brain might trigger or aggravate brain tumors or neurodegenerative diseases such as Parkinson's disease (PD). Aggregation of neural  $\alpha$ -synuclein (S) is central to PD pathophysiology, and invertebrate models expressing human S have helped elucidate factors affecting the aggregation process. We have recently developed a transgenic strain of *Caenorhabditis elegans* carrying two S constructs: SC tagged with cyan (C) blue fluorescent protein (CFP), and SV with the Venus (V) variant of yellow fluorescent protein (YFP). During S aggregation in these SC+SV worms, CFP, and YFP tags are brought close enough to allow Foerster Resonance Energy Transfer (FRET). As a positive control, S aggregation was promoted at low Hg<sup>2+</sup> concentrations, whereas higher concentrations activated stress-response genes. Using two different exposure systems described previously, we tested whether RF fields (1.0 GHz CW, 0.002–0.02 W kg<sup>-1</sup>; 1.8 GHz CW or GSM, 1.8 W kg<sup>-1</sup>) could influence S aggregation in SC+SV worms. YFP fluorescence in similar SV-only worms provided internal controls, which should show opposite changes due to FRET quenching during S aggregation. No statistically significant changes were observed over several independent runs at 2.5, 24, or 96 h. Although our worm model is sensitive to chemical promoters of aggregation, no similar effects were attributable to RF exposures. Bioelectromagnetics. 37:116–129, 2016. © 2016 Wiley Periodicals, Inc.

**Key words:** microwave fields;  $\alpha$ -synuclein aggregation; Foerster resonance energy transfer; mercury toxicity; *C. elegans* Parkinson's disease model

## INTRODUCTION

Controversy surrounding potential health risks of mobile telecommunications devices (both phones and masts) operating in the radiofrequency (RF) range has largely focused on whether prolonged exposures might increase risk of developing brain cancers [Hardell et al., 2007, 2013; Sage and Carpenter, 2009], although the international Interphone study concluded there is no such effect [INTERPHONE Study Group, 2010, 2011]. Hand-held devices are usually used in close proximity to the head, so RF fields might also affect normal brain functions [Abramson et al., 2009; Croft et al., 2010], or possibly initiation or progression of neurodegenerative diseases such as Parkinson's disease (PD) [Del Vecchio et al., 2009]. We have previously suggested that exposure to weak continuous wave (CW) RF fields at 1.0 GHz can promote in vitro aggregation of proteins such as

Grant sponsor: Nuffield Trust, London, United Kingdom.

Conflict of interest: None.

Current address of Archana Nagarajan: CORE Institute, University of Stavanger, Stavanger, Norway.

Current address of Mehri Kaviani Moghadam: Sir Peter Mansfield Imaging Center, School of Physics and Astronomy, University of Nottingham.

\*Correspondence to: David I. de Pomerai, School of Life Sciences, University of Nottingham, University Park, Nottingham NG7 2RD, United Kingdom. E-mail: ddepomerai@aol.com

Received for review 21 May 2015; Accepted 22 January 2016

DOI: 10.1002/bem.21959

Published online in Wiley Online Library (wileyonlinelibrary.com).

bovine serum albumin (BSA) and bovine insulin, the latter forming amyloid fibrils at high temperatures [de Pomerai et al., 2003], similar to those characteristic of neurodegenerative diseases such as PD. Similar effects on protein aggregation in vivo could also explain why heat-shock proteins (HSPs) are commonly induced by RF exposure [Daniells et al., 1998; de Pomerai et al., 2000; Leszczynski et al., 2002; Cotgreave, 2005], since these HSPs act as chaperones to refold misfolded, aggregation-prone cellular proteins and to disperse (or prevent formation of) protein aggregates. CW fields tested at 1.0 GHz are similar to (but not identical with) those generated by older analogue mobile phones, which normally operated at 918 MHz. However, a careful re-investigation of our *C. elegans* system concluded that reported induction of an *hsp-16.1* reporter was probably caused by a subtle thermal artefact (c. 0.2 °C), since when temperature differences between sham and RF-exposed conditions were minimized, there was no longer any detectable induction attributable to RF fields applied [Dawe et al., 2006], nor was there any major RF-induced change in the global gene expression profile [Dawe et al., 2009]. We also repeated these studies at a higher specific absorption rate (SAR), using a temperature-controlled Reflex sXc-1800 instrument, which generates much stronger RF fields at 1.8 GHz (either CW or global system for mobile telecommunications (GSM)) of up to 2 W kg<sup>-1</sup> as a model for standard GSM mobile phones, but again there was no discernible effect on *hsp-16.1::lacZ* expression [Dawe et al., 2008]. These findings suggested that our original protein aggregation data [de Pomerai et al., 2003] might also be influenced by thermal or other artefacts, but until recently we had no means of testing this possibility with an in vivo model in which protein aggregation could be monitored readily.

Several fluorescence techniques have been developed for studying protein-protein interactions (such as aggregation), including use of Foerster Resonance Energy Transfer (FRET) between cyan fluorescent protein (CFP) and yellow fluorescent protein (YFP). Typically, excitation of a CFP-labelled protein results in higher wavelength emissions that can in turn excite a neighbouring YFP-labelled protein to fluoresce at a still higher wavelength. However, this is only possible when CFP and YFP tags are in close proximity, normally within 70 Å [Gordon et al., 1998], a condition met within aggregates but not in free cytosolic solution. Aggregation of human protein  $\alpha$ -synuclein (S) in dopaminergic neurons of the substantia nigra plays a major role in causation and progression of PD, and may be linked to metal binding [Wright and Brown, 2008].

Synucleinopathies also include a range of other, rarer neurodegenerative diseases, including dementia with Lewy bodies (DLB) and multiple system atrophy (MSA) [McCann et al., 2014], widening the relevance of studies on S aggregation [Goedert, 2015]. We have recently published details of a double transgenic strain of *C. elegans* co-expressing two human S constructs [Bodhicharla et al., 2012; Nagarajan et al., 2015]: SC carrying a C-terminal CFP tag, and SV carrying a similar YFP (Venus) tag. Both transgenes are driven by separate *unc-54* myosin promoters, giving high-level expression in body-wall muscle, and henceforth this strain is abbreviated as *unc-54::SC+SV*. During aggregation of S, the attached CFP and YFP tags are brought into close proximity, allowing FRET between them. After correcting for cross-talk between channels, there remains a robust net FRET signal, which monitors S protein aggregation. This FRET signal increases significantly as worms get older [Bodhicharla et al., 2012], or following ribonucleic acid interference [RNAi] to knock down both *hip-1* and *hsp-70* expression simultaneously [Roodveldt et al., 2009; Nagarajan et al., 2015], as well as during exposure to pesticide chlorpyrifos (1.0 mg l<sup>-1</sup>) or low concentrations of Hg<sup>2+</sup> (2.5–5.0  $\mu$ g l<sup>-1</sup>) [Nagarajan et al., 2015].

Here, we apply this *C. elegans* PD model to monitor possible RF-induced  $\alpha$ -synuclein aggregation, so as to verify or refute our earlier in vitro findings [de Pomerai et al., 2003] under in vivo conditions, using similar CW exposures at 1.0 GHz at physiological temperatures (25 °C). Simultaneous RF and sham exposures were conducted on two transgenic *C. elegans* PD models: *unc-54::SC+SV* worms [Bodhicharla et al., 2012] to monitor S aggregation by FRET, and NL5901 worms carrying a similar *unc-54::SV* construct ( $\alpha$ -synuclein tagged with YFP only) [van Ham et al., 2008] to monitor levels of YFP fluorescence. Recent evidence suggests that fluorescence quenching due to FRET occurs in NL5901 control worms, resulting from absorption of YFP emissions by growing aggregates of the SV fusion protein [Kaminski Schierle et al., 2011]. Thus if genuine aggregation of fusion proteins is occurring in vivo, a comparison between SC+SV and NL5901 strains (as here) should show an increase in FRET signal for the former but a decrease in YFP signal for the latter. By contrast, instances where both FRET (SC+SV) and YFP (NL5901) signals increase or decline together are more plausibly explained in terms of altered *unc-54* promoter activity affecting expression levels of fluorescent fusion proteins. This overcomes one of the inherent limitations of using the NL5901 strain on its own to monitor S aggregation,

since many stressful conditions might also tend to inhibit transgene expression.

Based on our earlier findings, we would expect RF exposure to promote S aggregation, which should increase FRET in SC+SV worms but decrease YFP fluorescence in NL5901 (SV) worms. The null hypothesis is that there will be no consistent statistically significant ( $P \leq 0.05$ ) effect of RF exposure on either S aggregation (in *unc-54::SC+SV* worms) or YFP fluorescence (in NL5901 worms). Because SAR measurements and modelling indicate a fivefold range in SAR between corner (high) and centre (low) wells in the 24-well microplates used for exposure, it is feasible to look for dose-dependent effects in RF-exposed but not sham plates across this limited dose range. We have also tested effects of stronger RF fields (1.8 GHz; SAR  $1.8 \text{ W kg}^{-1}$ ) [Dawe et al., 2008], using a well-characterized Reflex sXc-1800 exposure system under either CW or GSM Basic conditions for 2.5, 24, or 96 h.

## MATERIALS AND METHODS

### Exposure and Dosimetry

Effects of weak RF fields (1.0 GHz, SAR range  $0.004\text{--}0.02 \text{ W kg}^{-1}$ ) were tested within two octahedral transverse electromagnetic (TEM) cells built in the Department of Electrical and Electronic Engineering at Nottingham University (United Kingdom). One was made of copper and the other plated with silver. They were incubated at  $25^\circ\text{C}$  side by side in the same incubator as described previously [Dawe et al., 2006, 2009]. Dosimetry of these cells is described in Figure 1. The Nottingham TEM cell cannot be used to test effects of stronger RF fields because of known heating artefact [Dawe et al., 2006].

We therefore extended our TEM cell findings by using the well-characterized Reflex sXc-1800 exposure system, as done previously [Dawe et al., 2008]. This system provides two superimposed exposure chambers, each with a sample holder for six replica 3.5 cm Petri dishes. The operator is blind as to which chamber is live and which is sham, until codes are broken subsequently. With a nominal SAR setting of  $2.0 \text{ W kg}^{-1}$  at 1.8 GHz (either CW or GSM Basic), previous dosimetry [Dawe et al., 2008] suggested average SAR of  $1.8 \text{ W kg}^{-1}$  experienced by worms at the bottom of Petri dishes used for exposure. All details of the Reflex exposure system and dosimetry were exactly as described previously [Dawe et al., 2008], except that GSM Basic rather than GSM Talk-mode was employed here. Induced H-fields were approximately  $1.6 \text{ A m}^{-1}$  and orthogonal to induced

E-field, both of which were predominantly parallel to the bottom of the dish. At the applied SAR of  $1.8 \text{ W kg}^{-1}$ , the temperature load was  $<0.1^\circ\text{C}$ ; non-uniformity at the bottom of the dish was estimated at 23% and relative variability between Petri dishes across the six-dish sample holders at less than 5% [Schuderer et al., 2004]. Ambient ELF exposure within the housing incubator was approximately  $5 \mu\text{T}$  rms, but this would be experienced equally by both sham and exposed samples. In both exposure chambers, half the Petri dishes were randomly allocated to contain NL5901 worms and the other half SC+SV worms.

### Worm Culture

This study used the double-transgenic *unc-54::SC+SV* strain [Bodhicharla et al., 2012; Nagarajan et al., 2015], together with a control strain, NL5901 (donated by Aamir Nazir, Central Drug Research Institute, Lucknow, India). NL5901 carries a similar S construct fused to YFP (V), driven by the same *unc-54* myosin promoter, and has been used previously in RNAi screening for genes affecting S aggregation [van Ham et al., 2008, 2010; Roodveldt et al., 2009]. Here, YFP fluorescence in NL5901 worms monitors both activity of the *unc-54* promoter and extent of S aggregation through quenching of YFP signal due to FRET [Kaminski Schierle et al., 2011]. We have also used transgenic reporter strains expressing green fluorescent protein (GFP) fusion constructs to monitor the activity of three classic stress-response genes [Anbalagan et al., 2012, 2013], namely: *hsp-16.2::GFP* (CL2070) [Link et al., 1999], *mtl-2::GFP* (BC20342), and *sod-4::GFP* (BC20333); these last two strains were supplied through the Baillie GFP Genome Project at Simon Fraser University (Burnaby, Canada).

Worms were cultured as described previously [Dawe et al., 2006] at  $20^\circ\text{C}$  on nematode growth medium (NGM) agar plates with *E. coli* as food, and synchronized by filtering suspensions of mixed-stage worms in K medium (53 mM NaCl, 32 mM KCl) [Williams and Dusenbery, 1990] through a  $5 \mu\text{m}$  mesh, allowing only L1 larvae to pass through [Mutwakil et al., 1997]. Larvae were pelleted and cultured on fresh plates to the L4 stage (2 d at  $20^\circ\text{C}$ ). After washing and resuspending in K medium, worms were stirred during dispensing into 24 well plates (Nunc, Roskilde, Denmark) so that each well received essentially equal numbers ( $\pm 5\%$ ) of worms in a  $50 \mu\text{l}$  aliquot. For  $\text{Hg}^{2+}$  exposures, worms of all five strains were incubated for 24 h at  $20^\circ\text{C}$  with  $\text{Hg}^{2+}$  at concentrations ranging from 0 to  $10 \mu\text{g l}^{-1}$  for *unc-54::SC+SV* and NL5901 (Fig. 2A), and from

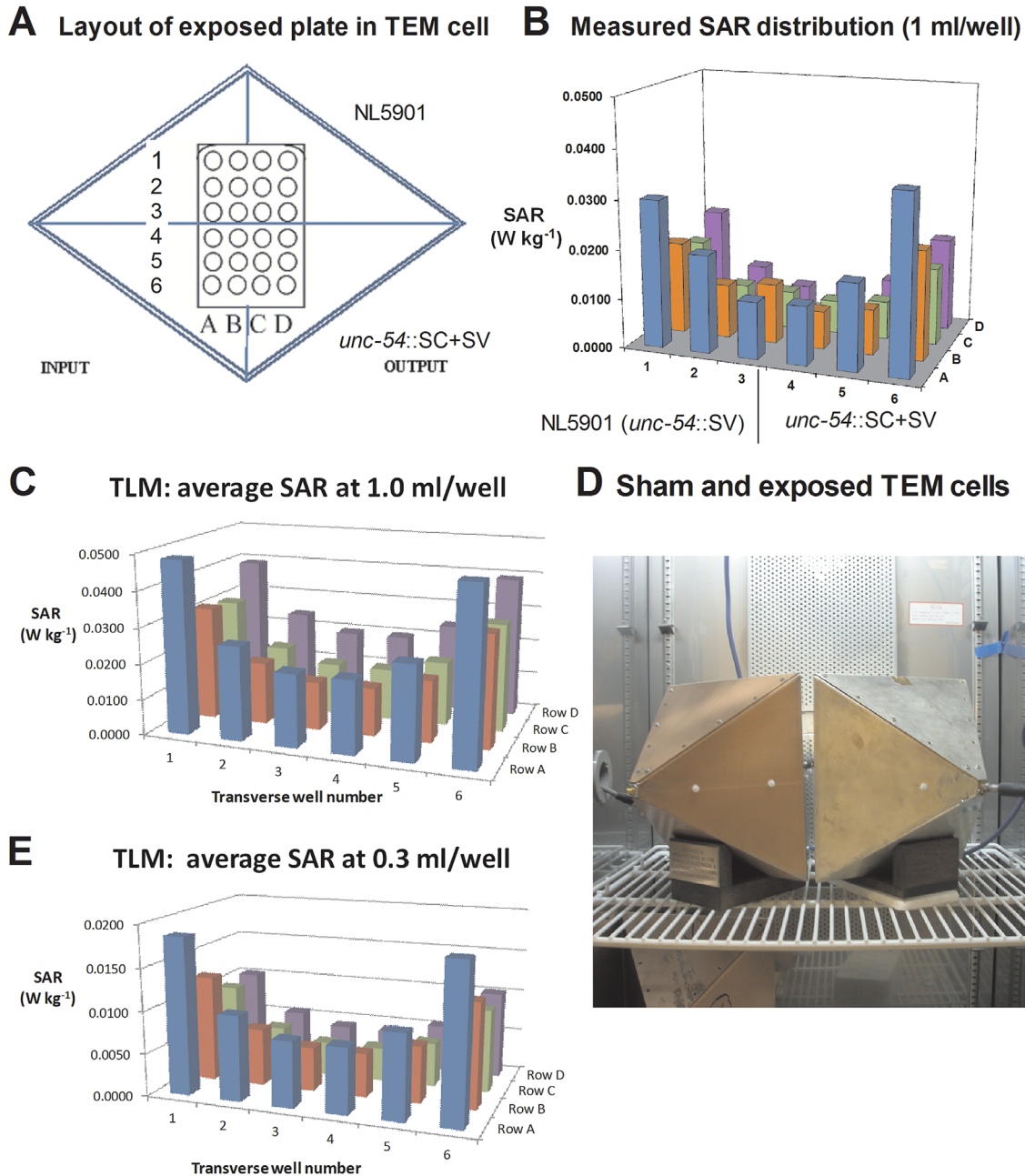


Fig. 1. Dosimetry of RF fields. (A) Schematic of 24-well plate layout within TEM cell. Measured (B) and TLM-modelled (C) SAR distributions for a 24-well plate loaded with 1.0 ml per well of K medium. (D) Both sham (copper, on left) and exposed (silver-plated, on right) TEM cells were located side by side within incubator. (E) Corresponding TLM-modelled SAR distribution with 0.3 ml of K medium per well.

0 to 400  $\mu\text{g l}^{-1}$  for GFP stress-reporter strains (Fig. 2B). All wells contained 300  $\mu\text{l}$  final volume, and GFP fluorescence was measured in the loose worm pellet after cooling on ice [Anbalagan et al., 2012, 2013]; means derived from quadruplicate exposures were divided by the corresponding zero control mean (no  $\text{Hg}^{2+}$ ;  $n = 4$ ) and multiplied by 100, giving

a normalized percentage expression (NPE) relative to controls (100%).

#### RF Exposures Using Nottingham TEM Cell

For this purpose, 50  $\mu\text{l}$  aliquots of synchronized NL5901 worms were mixed with 250  $\mu\text{l}$  of K medium per well in rows 1–3 of the plate (upper half in

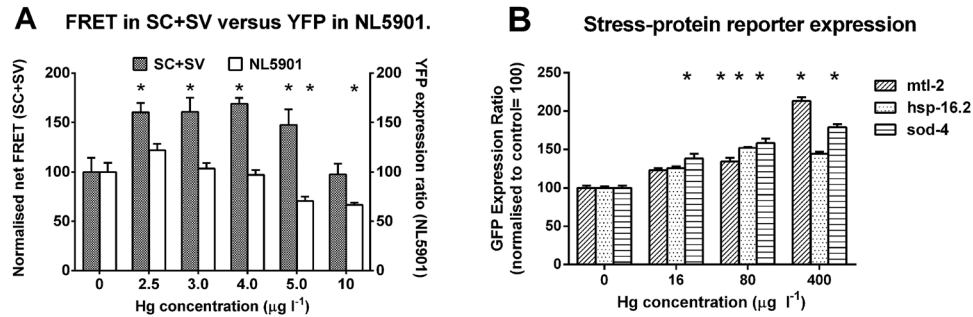


Fig. 2. Effects of  $\text{Hg}^{2+}$  (positive control) on FRET and reporter expression in *C. elegans*. (A) Responses of transgenic S-expressing worms to various concentrations of  $\text{Hg}^{2+}$ : shaded bars (left in each pair) show net FRET in *unc-54::SC+SV* worms, while open bars (right) show YFP fluorescence in NL5901 (*unc-54::SV*) worms. (B) responses of three stress-inducible GFP reporter strains to  $\text{Hg}^{2+}$ : within each group of three bars, that on the left (hatched) shows *mtl-2*, that in the centre (stippled) *hsp-16.2*, and that on the right (horizontal shading) *sod-4*. All data in both parts were normalized against corresponding K medium controls with zero Hg (expression ratio 100). Asterisks indicate statistically significant ( $P < 0.05$ ) differences from these zero Hg controls.

Fig. 1A, left-hand side in Fig. 1B, C, and E). Similarly, synchronized *unc-54::SC+SV* worms were aliquoted into rows 4–6 of the plate (lower half in Fig. 1A, right-hand side in Fig. 1B, C, and E). Because SAR distribution is not quite symmetrical, SAR scales for each strain do not coincide, although they largely overlap. Since no RF field was applied to sham controls, well position was measured symmetrically as mean distance from the plate centre, which broadly correlates with SAR (Fig. 1B, C, and E). Exposed and sham plates were incubated at  $25^\circ\text{C}$  ( $\pm 0.2^\circ\text{C}$ ) for 2 h initially, then after measuring YFP fluorescence (NL5901) or FRET signal (*unc-54::SC+SV*), all well contents were returned to their source wells and incubation continued overnight at  $25^\circ\text{C}$ , followed by a second set of readings at 24 h. For fluorescence determinations, well contents were transferred into black non-fluorescent 96-well U-bottomed microplates (Nunc 267342, Roskilde, Denmark) and stood on ice for 15 min to allow worms to settle, then fluorescence in the pellet was measured in a Perkin Elmer Victor 1420 Multilabel counter (PerkinElmer, Seer Green, UK). For GFP, narrow band-pass filters were used at 485 nm for excitation and 525 nm for emission; for CFP and YFP, filters used were at 433 and 510 nm, respectively, for excitation, and at 486 and 533 nm, respectively, for emission. For FRET studies, excitation was at 433 nm (as for CFP), and emissions were read at 533 nm (as for YFP); FRET readings were corrected for fluorescence cross-talk in a parallel, equimolar mixture of YFP and CFP, and in wells containing YFP fusion alone or a CFP fusion alone, as described previously [Bodhicharla et al., 2012; Nagarajan et al., 2015].

Data from each of three to seven independent runs were normalized against mean sham control values for each run (set arbitrarily at 100; cf. NPE above) in order to establish a common baseline for all runs.

#### RF Exposures Using Reflex sXc-1800 System

Each six-place sample holder contained three randomly arranged 3.5 cm Petri dishes (Nunc) each containing c. 3000 NL5901 worms in a total volume of 2.0 ml K medium, while the other three dishes contained a similar number of SC+SV worms in the same total volume of K medium. Each 3.5 cm dish was sealed with a narrow strip of Parafilm to prevent excessive evaporation during long-term exposures. Synchronized L4 worms (as above) were used for 2.5 and 24 h time-points in this study, whereas non-synchronized mixed-stage cultures of worms were used at 96 h exposures, since synchrony was inevitably lost after  $>24$  h when L4 larvae mature to adults and start to reproduce. Exposures were conducted at  $25^\circ\text{C}$  for 2.5, 24, or 96 h; longer exposures were not feasible because of the Reflex instrument's 400,000 s maximum time setting. The worm suspension from each dish was split equally between six wells of a 96-well U-bottomed black non-fluorescent plate (as above), cooled on ice, and either FRET (for SC+SV) or YFP (for NL5901) was measured as above. The mean of all six readings provided a representative single measure of FRET or YFP signal for each dish. Three such replica dishes were available for each strain in each chamber (later identified as sham or exposed), and three to seven runs were conducted for each time point (2.5, 24, or 96 h) and field type (GSM Basic or CW). For statistical purposes, three replicates

within each run were treated as pseudo-replicates, and run means ( $n = 3-7$ ) as true replicates.

### Statistical Analysis

Responses to  $\text{Hg}^{2+}$  were analyzed using one-way ANOVA with Dunnett's multiple comparisons test (Fig. 2).

For RF experiments using Nottingham TEM cells, linear regression lines were fitted (using GraphPad Prism version 6.04; La Jolla, CA) to normalized mean data derived from all three runs in each panel of Figure 3. However, in statistical analysis the three runs were kept separate. Fixed effects of treatment (exposed vs. sham) and of SAR dose (or distance from centre), and their interaction, were tested separately at each time point for YFP (NL5901) and FRET (*unc-54::SC+SV*) using general linear mixed effects models fitted with the nlme package in R version 2.15.1 [R Core Team, 2014]. A random effect of run was included in the models to account for random variation in responses among runs. Models were simplified by backwards deletion of fixed effects from a saturated model fitted using maximum likelihood; significance was assessed using likelihood ratio (LR) tests [Zuur et al., 2009].

A different analysis was performed on Reflex sXc-1800 data for both SC+SV and NL5901 strains under sham vs. GSM or CW exposure conditions at each of the three time-points (2.5, 24, and 96 h), using raw rather than normalized data. This is because the data normalization process converts all sham means to 100%, removing variability within this data set (see Fig. 4). Effects of treatment (exposed vs. sham), strain and field type (plus their interactions) on expression levels were analyzed using three-way ANOVA in R version 3.0.1 [R Core Team, 2014]. Expression levels were averaged across pseudoreplicates prior to analysis. Model checking confirmed that assumptions of normality and homogeneity of variance were valid. Analysis was conducted using raw data, but for clarity we have plotted treatment data normalized relative to sham controls in Figure 4.

## RESULTS

### Dosimetry of Nottingham TEM Cell

Figure 1 shows layout and dosimetry of Nottingham TEM cell exposure system used here and in previous studies [Dawe et al., 2006, 2009]. CW RF field at 1.0 GHz and 0.5 W was applied to the silver-plated cell, its copper companion acting as a sham control (no field). Measured temperature differences between exposed and sham cells were no greater than

0.15 °C with a 1.0 W power input, double the 0.5 W used both here and previously [Dawe et al., 2006, 2009]. Plastic 24-well plates (Nunc) were placed centrally on the septum, as shown schematically in Figure 1A. Finite-difference time-domain (FDTD) modelling of SAR distribution in 24-well plates loaded with 1.0 ml per well of K medium suggested a range of 0.004–0.04  $\text{W kg}^{-1}$  [Dawe et al., 2009], in close agreement with actual field measurements using an isotropic IndexSAR IXP-010 E-field probe (IndexSAR Instruments, Newdigate, UK) dipping into the medium, conducted at the UK National Physical Laboratory [Dawe et al., 2006, 2009], as shown in Figure 1B. However, in the present study, each loaded well contained only 0.3 ml of K medium, a practical limitation imposed by the 300  $\mu\text{l}$  well capacity of 96-well non-fluorescent U-bottomed black plastic microplates used for fluorescence measurements. Transmission Line Modelling (TLM) [Christopoulos, 2006] was used to model SAR distribution in plates loaded with 1.0 ml per well of K medium (Fig. 1C), using the exposure apparatus described above and illustrated in Figure 1D. Figure 1E shows similar modelling of SAR in plates loaded with 0.3 ml per well. TLM predictions of SAR for 1.0 ml sample volumes (0.004–0.04  $\text{W kg}^{-1}$ ; Fig. 1C) were in close agreement with actual field measurements (Fig. 1B), consistent with previous findings [Paul et al., 1999, 2002], and were approximately twofold greater than for 0.3 ml samples (0.002–0.02  $\text{W kg}^{-1}$ ; Fig. 1E) We therefore used TLM-predicted SAR values for 0.3 ml samples (Fig. 1E) when preparing Figure 3 and conducting statistical analyses.

### Positive Controls Using Mercury

Figure 2A is a positive control to demonstrate sensitivity of the FRET signal for monitoring aggregation of  $\alpha$ -synuclein (S) moieties. It shows responses to low (0–10  $\mu\text{g l}^{-1}$ ) concentrations of  $\text{Hg}^{2+}$  both for FRET (measuring S aggregation) in *unc-54::SC+SV* worms, and for YFP fluorescence in control NL5901 worms. FRET signals increased by nearly twofold ( $P < 0.05$  for 2.5–5.0  $\mu\text{g l}^{-1}$   $\text{Hg}^{2+}$ ), whereas YFP fluorescence increased slightly initially ( $P > 0.05$ ) and then decreased sharply by twofold ( $P < 0.05$ ; Fig. 2A); interestingly, these responses faded out at higher  $\text{Hg}^{2+}$  concentrations ( $\geq 10 \mu\text{g l}^{-1}$ ). Figure 2B shows induction by  $\text{Hg}^{2+}$  of three GFP reporters representing classic stress-response genes, namely *hsp-16.2* (a highly inducible small heat shock protein) [Link et al., 1999], *mtl-2* (a metal-inducible metallothionein) [Swain et al., 2004], and *sod-4* (an inducible extracellular superoxide dismutase) [Anbalagan et al., 2012]. The lowest  $\text{Hg}^{2+}$  concentration able to induce these three GFP reporters

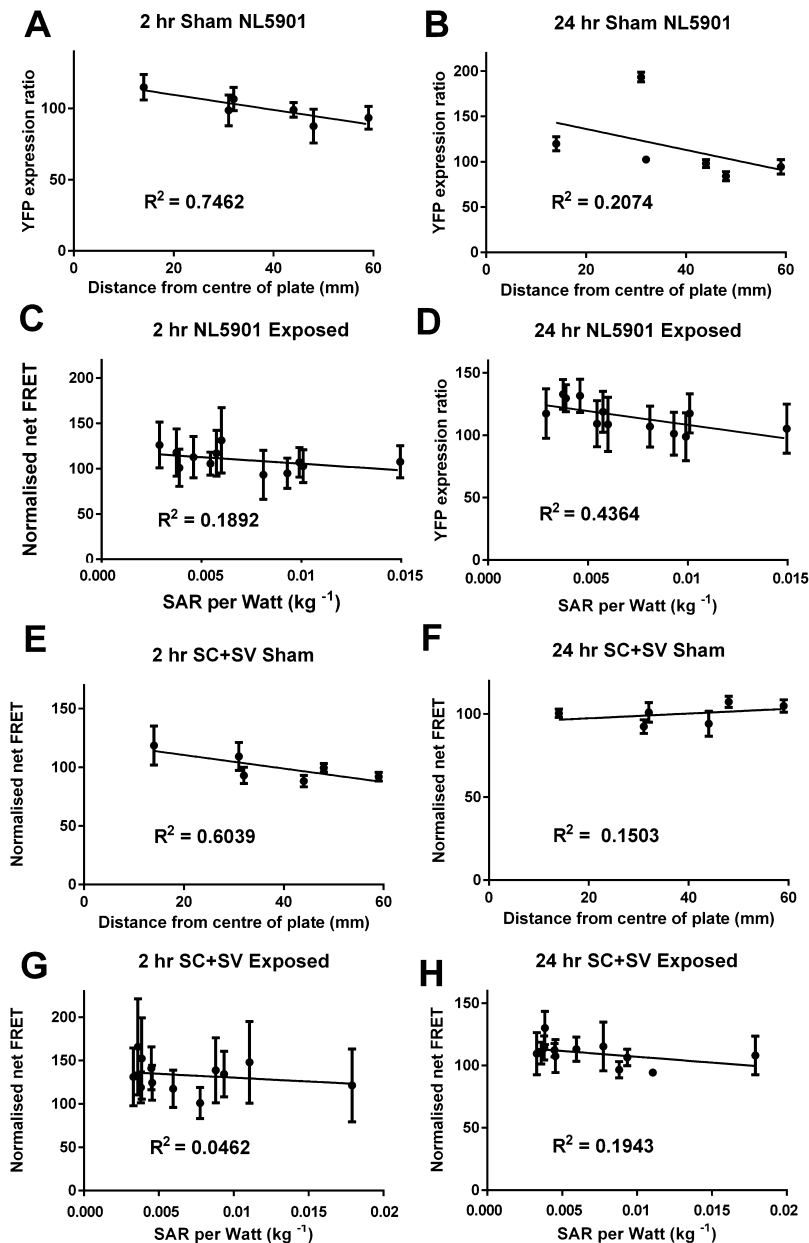


Fig. 3. YFP expression and FRET in transgenic *C. elegans* exposed to weak CW RF fields at 1.0 GHz. For this composite figure, both YFP expression in NL5901 worms (parts **A-D**) and net FRET in *unc-54::SC+SV* worms (parts **E-H**) were plotted against distance from centre of plate (sham only; parts **A, B, E, and F**) or SAR per 0.3 ml (exposed only; parts **C, D, G, and H**). Means and SEMs were calculated from three independent runs at both 2 h (parts **A, C, E, and G**) and 24 h (parts **B, D, F, and H**), and data were normalized against corresponding sham controls as 100%. Linear regression analysis was performed on each data set, and  $R^2$  values are stated on each panel.

was  $16 \mu\text{g l}^{-1}$  ( $P < 0.05$  for *sod-4*), but *mtl-2* was induced by twofold only at  $400 \mu\text{g l}^{-1}$  ( $P < 0.05$ ).

#### RF Exposures Using Nottingham TEM Cell

In Figure 3, well position (distance from plate centre) was used as a surrogate variable when plotting

sham data, since SAR cannot be used because no field was applied in this cell. It is conceivable, though highly unlikely, that artefacts such as heat radiating from TEM cell walls might affect corner wells (closest) more than central wells (most distant). Plotting sham data on this surrogate distance scale

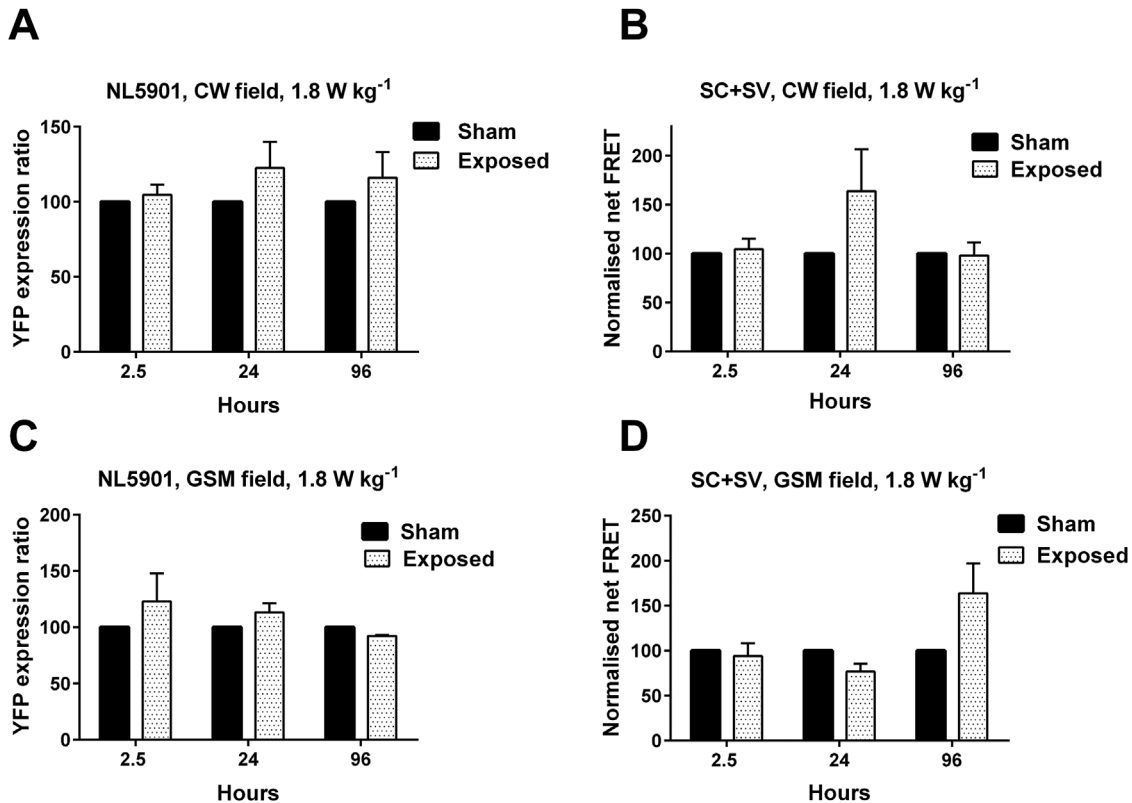


Fig. 4. YFP expression and FRET in transgenic *C. elegans* exposed to 1.8 GHz RF fields. SC+SV and NL5901 worms were exposed to 1.8 GHz CW or GSM-Basic RF fields in a Reflex sXc-1800 exposure system. All data from exposed samples were normalized against corresponding sham means (as 100). Three to seven independent runs were performed for each time point (2.5, 24, or 96 h) and field type (CW in parts **A** and **B**, GSM Basic in parts **C** and **D**). Mean and SEM data are shown for YFP fluorescence in NL5901 worms in parts **A** and **C**, and for net FRET in SC+SV worms in parts **B** and **D**. Each panel compares responses at all three time points for sham exposures (filled columns; mean = 100 throughout as used for normalization) and RF exposures (stippled columns  $\pm$  SEM bars).

(which is symmetrical, unlike SAR distribution) should reveal any such artefactual trends in the level of response when compared against corresponding RF-exposed data.

In Figure 3, normalized YFP fluorescence in NL5901 worms is shown in Figure 3A–D, with sham controls in Figure 3A and B (at 2 and 24 h) and exposed samples in Figure 3C and D (at 2 and 24 h). Similarly, corrected and normalized net FRET values for the *unc-54::SC+SV* strain are shown in Figure 3E–H, with sham controls in Figure 3E and F (2 and 24 h) and exposed samples in Figure 3G and H (2 and 24 h). Statistical analysis of YFP expression in NL5901 worms indicated significant effects of RF treatment (LR 10.69,  $P=0.001$ ; 1 d.f.) and SAR (LR 8.804,  $P=0.003$ ; 1 d.f.) at 24 h, but not at 2 h (LR 2.60,  $P=0.103$  for treatment; LR 2.58,  $P=0.108$  for SAR; 1 d.f. for both). At neither 2 h (LR 0.034,

$P=0.853$ ) nor 24 h (LR 0.028;  $P=0.866$ ) was there any significant interaction between RF treatment and SAR. For the *unc-54::SC+SV* strain, statistical analysis suggested a significant effect of SAR (LR 5.170,  $P=0.023$ ; 1 d.f.) but not of RF treatment (LR 0.016,  $P=0.898$ ; 1 d.f.) at 2 h, but at 24 h there was no effect of either (LR 0.013,  $P=0.910$  for RF treatment; LR 2.414,  $P=0.12$  for SAR; 1 d.f. for both), and no interaction between them (LR 0.000078,  $P=0.993$  at 2 h, 1 d.f.; LR 0.439,  $P=0.508$  at 24 h, 1 d.f.).

Most regression lines fitted to data in Figure 3 show a slight negative trend, with the sole exception of the sham data for SC+SV at 24 h.  $R^2$  values are given in each part of Figure 3 for regression lines plotted, but in only two cases (2 h sham for NL5901 in part A, and 24 h exposed for NL5901 in part D) did these slopes differ significantly from zero ( $P=0.0266$  for part A;  $P=0.0194$  for part D).

### Exposures Using the Reflex sXc-1800 System

Figure 4 illustrates changes in YFP fluorescence for NL5901 worms (Fig. 4A and C) and in FRET for *unc-54::SC+SV* worms (Fig. 4B and D) after exposure to CW or GSM fields for 2, 24, or 96 h. At 24 h, CW-exposed SC+SV worms showed apparently elevated FRET, as was also seen for GSM-exposed SC+SV worms at 96 h; however, both increases were associated with large standard errors.

Statistical analysis of raw data underlying Figure 4 using three-way ANOVA (Table 1) showed no significant main effect of treatment (vs. sham) or of field (CW or GSM Basic), with *P* values ranging from 0.434 (treatment at 2.5 h) to 0.962 (treatment at 96 h). However, there was a highly significant effect of strain (*P* = 0.00074 at 96 h, much lower at 2.5 or 24 h), due largely to order-of-magnitude numerical differences between net FRET (ranging from 100 to 2,000) and YFP measurements (4,000–15,000) in raw data-sets used. Interaction terms (treatment:field, treatment:strain, field:strain or treatment:field:strain) did not approach significance (*P* ranging from 0.366

to 0.971). Overall, no statistically significant effects (other than strain) were identified.

## DISCUSSION

### Study Limitations

We have examined only a limited parameter space in terms of range of test exposures to electromagnetic fields (EMFs). We initially used 1.0 GHz CW RF fields at low SAR (0.5 W power input; SAR range 0.002–0.02 W kg<sup>-1</sup>) generated in the Nottingham TEM cell described previously [de Pomerai et al., 2000, 2003; Dawe et al., 2006, 2009] at 2 and 24 h time-points, using synchronized L4 and young adult transgenic worms. This system provides an approximate model for older analogue mobile phones operating at 900 Mz. The only deviation from our previous studies was reduction in sample volume from 1.0 to 0.3 ml per well, a restriction imposed by the well capacity of 96-well microplates; this reduced TLM-modelled SAR by about 50% (Fig. 1C and E). These specific exposure conditions (using 1.0 ml samples)

**TABLE 1. Statistical Analysis of Reflex sXc-1800 Data Shown in Figure 4**

	Error DF	Df	SS	MS	F	<i>P</i>
2.5 h						
Treatment	23	1	2397176	2397176	0.6358	0.4342
Field	22	1	958001	958001	0.245	0.626
Strain	24	1	5.43E + 08	5.43E + 08	146.33	3.41E-11
Treatment:field	20	1	959600	959600	0.2338	0.6346
Treatment:strain	21	1	3377250	3377250	0.8574	0.3661
Field:strain	19	1	114955	114955	0.0265	0.8726
Treatment:field:strain	18	1	2093913	2093913	0.4674	0.5039
R-squared:	86.93%					
24 h						
Treatment	23	1	753331	753331	0.1218	0.7288
Field	22	1	2903643	2903643	0.4637	0.4996
Strain	24	1	5.76E+08	5.76E + 08	80.5697	6.26E-13
Treatment:field	20	1	594287	594287	0.0921	0.7631
Treatment:strain	21	1	4311272	4311272	0.6834	0.4132
Field:strain	19	1	604462	604462	0.0916	0.7638
Treatment:field:strain	18	1	13817	13817	0.002	0.9642
R-squared:	69.53%					
96 h						
Treatment	23	1	11500	11500	0.0023	0.9624
Field	22	1	1836443	1836443	0.3518	0.5591
Strain	24	1	72571937	72571937	14.928	0.000743
Treatment:field	20	1	21902	21902	0.0038	0.9514
Treatment:strain	21	1	7379.8	7379.8	0.0013	0.971
Field:strain	19	1	2645971	2645971	0.4483	0.5112
Treatment:field:strain	18	1	163132	163132	0.0262	0.8732
R-squared:	38.35%					

Statistical parameters derived from raw data on which Figure 4 is based (before normalization). Three-way ANOVA was conducted to examine possible effects of treatment (sham vs. RF), field type (CW vs. GSM Basic) or strain (NL5901 vs. SC + SC). MS = mean squares; SS = sum of squares; R-squared gives percentage of total variability from each factor.

were reported to increase *C. elegans* growth and *hsp-16.1::lacZ* transgene expression at 26 °C [de Pomerai et al., 2000], and promoted aggregation of bovine insulin at 60 °C and of BSA at 37 °C [de Pomerai et al., 2003]. We have already shown that reported effects on *C. elegans hsp-16.1* reporter expression resulted from a thermal artefact caused by power leakage and slight heating (c. 0.15 °C), which could be largely abolished by modifications of the TEM cell [Dawe et al., 2006]. Our present study using the modified TEM cell for RF exposure was designed to test whether similar CW RF fields can promote protein aggregation in vivo, based on a novel FRET-based assay in transgenic *unc-54::SC+SV* worms [Bodhicharla et al., 2012; Nagarajan et al., 2015].

Using this exposure system, it is not possible to increase SAR by boosting power input into the TEM cell, since this causes substantial sample heating [Dawe et al., 2006]. A different exposure system with built-in air cooling, such as the Reflex sXc-1800, was therefore needed to investigate effects of much higher SAR [Dawe et al., 2008]. We used this system to investigate effects of 1.8 GHz fields (both CW and GSM Basic) at an estimated SAR of 1.8 W kg<sup>-1</sup> over time periods ranging from 2.5 to 96 h, modelling fields generated by standard GSM mobile phones. However, there were practical limitations on duration and timing of worm exposures to RF. We found that background FRET signal increases with age in synchronized cultures of *unc-54::SC+SV* worms, approximately doubling over a week from L4 larvae to six-day adults [Bodhicharla et al., 2012], which is consistent with increased aggregation of cellular proteins in older worms [David et al., 2010]. Synchronization of worms by egg isolation or L1 filtration [Mutwakil et al., 1997] is straightforward, but synchrony is lost once adults start reproducing after 24–30 h, unless this process is blocked by using sterile mutants or toxic anti-mitotic drugs such as 5-fluorodeoxyuridine (FUdR) [Mitchell et al., 1979], either of which would introduce further confounding effects. For this reason, mixed-stage non-synchronized cultures were used for the longest (96 h) exposures. Despite caveats above, age-related changes in FRET and/or YFP should affect both exposed and sham-treated worms equally, and such changes are corrected for during data normalization for Figure 4, because the sham mean is used as denominator for the RF-exposed data at each time point. Petri dishes were checked microscopically before taking fluorescence readings, and in all cases >80% of worms (adults and larvae) were still wriggling actively after 96 h, with no apparent differences between RF-exposed and sham conditions.

It is important to establish that fluorescence changes measured here reflect actual changes in S transgene expression and/or fusion-protein aggregation. Detailed evidence on this point is provided by van Ham et al. [2010] for NL5901, and we have used real-time quantitative PCR for SC+SV to show that both transgenes are co-expressed at similar levels, which decrease markedly over time between L4 larvae and six-day adults despite a twofold increase in FRET due to S aggregation [Nagarajan et al., 2015]. This increase in FRET days after a decline in transgene expression also suggests that fusion proteins are stable. We have shown that S fusion proteins extracted from SC+SV worms are of expected size (c. 47 kDa) and are relatively stable—without becoming extensively cleaved or degraded over timescales of order of days [Nagarajan et al., 2015], thereby justifying our focus in this study on three widely separated time-points (2.5, 24, and 96 h).

One further limitation of the FRET assay described here is that data normalization can potentially introduce an additional artefact in runs where sham control readings are unusually low, disproportionately magnifying any effect of applied treatments. This is exemplified by the higher means and large error bars seen for SC+SV with CW exposure over 24 h (Fig. 4B), and with GSM exposure over 96 h (Fig. 4D). The problem here arises from sensitivity of the normalization procedure to the sham mean (which is the denominator used for all FRET calculations), and can best be addressed by increasing numbers of replica runs. Such results are best interpreted with caution, pointing to the large variance rather than elevated mean. Since both Hg<sup>2+</sup> (Fig. 2A) and the pesticide chlorpyrifos [Nagarajan et al., 2015] induce two to threefold increases in FRET for SC+SV worms and corresponding decreases in YFP fluorescence for NL5901 worms, availability of monomeric fusion proteins is unlikely to be a limiting factor in RF studies presented here.

There is evidence that non-thermal RF bioeffects may be non-linear, often occurring within narrow windows of frequency, dose, and exposure time [Adey, 1993]. Even so, such effects should still be robust and reproducible under identical experimental conditions, otherwise they are properly regarded as flukes rather than scientific findings. We have identified few if any robust effects (apart from that of Hg<sup>2+</sup>) in this study, and none which implicate RF fields as promoters of S aggregation. However, several caveats are in order. First, our *C. elegans* model measures S aggregation in body-wall muscle rather than in dopaminergic neurons (as in human PD), where additional neuronal factors and oxidative

stress may be important. Second, although S aggregation is sensitive to metals such as  $\text{Hg}^{2+}$  (Fig. 2A), this sensitivity may not extend to other potential stressors such as EMFs. There is still no widely accepted non-thermal mechanism for transducing EMF signals into measurable biological responses, even where these seem to occur reproducibly [Leszczynski et al., 2012]. Third, our experiments involved acute (2.5, 24, and even 96 h) RF exposures, but chronic exposure throughout the worms' 14–21 day lifespan might be more appropriate for assessing RF risk factors contributing to late-onset neurodegenerative diseases such as PD. For technical reasons discussed earlier, longer exposures present logistical difficulties. Fourth, nematodes are far removed from humans in phylogenetic terms—and therefore a lack of response in *C. elegans* does not necessarily mean that there would be no response whatsoever in humans. In particular, some signal-transducing systems and many anatomical features characteristic of vertebrates (e.g., the blood-brain barrier) are absent from *C. elegans*.

Given near-universal adoption of mobile telecommunications technologies across the world, even slight adverse effects of exposure to RF fields in biological model systems could have significant implications for public health. Epidemiological evidence for a role of such fields in promoting or initiating specific cancers (such as gliomas or acoustic neuromas) remains ambiguous and hotly contested [Hardell et al., 2007; Schleofer et al., 2007; Sage and Carpenter, 2009; INTERPHONE Study Group, 2010, 2011; Carlberg and Hardell, 2012; Hardell et al., 2013]. Equally, evidence for any role of EMFs in causation or aggravation of human neurodegenerative or psychiatric diseases remains scarce, although cognitive impairment associated with increased permeability of the blood-brain barrier in rodents following long-term exposure to 900 MHz GSM fields has been reported by two independent studies [Nittby et al., 2008, 2009; Tang et al., 2015]. A suggested link between increased EMF exposure and autism [Ahuja et al., 2013] rested largely on correlation and indirect associations, but no direct experimental evidence was adduced. Reported effects of RF fields on DNA damage in vivo [Deshmukh et al., 2013], or of pulse-modulated X-band microwave fields on astrocytoma cell proliferation [Perez-Castejon et al., 2009] were only indirectly associated with risk of neurodegenerative disease. Elsewhere, possible links with RF exposure are reviewed by several authors [Consales et al., 2012; Kesari et al., 2013; Gherardini et al., 2014], and with extremely low frequency (ELF) EMF exposure by Mattsson and Simko [2012], but there is a dearth of direct experimental evidence. Whereas

electromagnetic pulse exposure increased  $\beta$ -amyloid expression in rats [Jiang et al., 2013], long-term exposure to 918 MHz GSM RF fields reportedly reversed  $\beta$ -amyloid deposition in a transgenic mouse model of Alzheimer's disease [Arendash et al., 2012]. Similarly, 900 MHz GSM fields caused only modest increases in constitutive HSP70 and HSP90 expression and concomitantly decreased  $\alpha$ -synuclein expression, all of which were attributable to a  $0.5^\circ\text{C}$  increase in temperature [Terro et al., 2012]. Recent reports using long-term ELF EMF exposures suggest these did not aggravate disease in mouse models of Alzheimer's or amyotrophic lateral sclerosis [Liebl et al., 2015], and improved both spatial memory disorder and hippocampal damage in a rat model of Alzheimer's [Liu et al., 2015]. Further studies of EMF effects in tractable models of human neurodegenerative diseases are urgently needed, and any robust effects reported will require exact replication by several independent laboratories.

The present in vivo study investigated modulation of S aggregation in an eminently tractable *C. elegans* PD model by weak 1.0 GHz CW RF fields across a low dose range ( $0.002$ – $0.02 \text{ W kg}^{-1}$  SAR), and by 1.8 GHz CW and GSM Basic fields at  $1.8 \text{ W kg}^{-1}$  [Dawe et al., 2008]. RF fields tested here neither significantly promoted nor inhibited S aggregation, and notably we failed to confirm our previous report that exposure to weak CW RF fields can exacerbate protein aggregation in vitro [de Pomerai et al., 2003]. Similar experiments are also feasible in vertebrate cell cultures expressing transfected  $\alpha$ -synuclein fusion constructs, allowing FRET or fluorescence recovery after photobleaching (FRAP) measurements of S aggregation [Roberti et al., 2011] in model systems closer to human biology.

## CONCLUSION

We used the toxic metal  $\text{Hg}^{2+}$  as a positive control to demonstrate sensitivity of *unc-54::SC+SV* worms for monitoring S aggregation (Fig. 2A), showing that FRET increased significantly at concentrations far lower than those needed to induce classical stress genes providing increased repair capacity (Fig. 2B). This raised the intriguing possibility that metals such as  $\text{Hg}^{2+}$  might promote S aggregation only at very low concentrations. As  $\text{Hg}^{2+}$  concentrations increased further, protective stress responses were induced, which would repair protein damage or prevent aggregation (heat shock proteins), sequester toxic metals (metallothioneins), and counter oxidative stress (superoxide dismutases) [Anbalagan et al., 2012]—thereby reducing metal-induced toxicity. Thus

our novel FRET assay affords a sensitive biomarker for S aggregation that seems well-suited to high-throughput screening assays, especially when the SC+SV strain is used in conjunction with NL5901.

Figure 3 shows dose responses at 2 and 24 h to CW RF fields across a limited SAR range both for FRET in SC+SV worms and for YFP fluorescence in NL5901 worms. In all cases but one, linear regression lines fitted to data showed a slight negative slope, which did not differ significantly from zero except in cases of sham-exposed NL5901 worms at 2 h (Fig. 3A), and of RF-exposed NL5901 worms at 24 h (Fig. 3D). In neither instance was there any sign of an opposite trend in the corresponding SC+SV data (Fig. 3E and H), arguing against any effect on S aggregation. Turning to data presented in Figure 4, there was again no statistical evidence for any significant effect of RF exposure on S aggregation in SC+SV or NL5901 worms (Table 1). This was true both for CW and GSM Basic fields at a much higher SAR ( $1.8 \text{ W kg}^{-1}$ ). Therefore, within the constraints of this study (in terms of time points and RF doses tested, and limited number of replica runs), we can find no convincing evidence to suggest that RF exposure can promote or inhibit S aggregation, and thereby aggravate or reduce risk of PD or other synucleinopathies.

**Note added in proof:** The double transgenic strain designated *unc-54::SC+SV* utilised throughout this study has now been deposited as strain DDP1 with the *Caenorhabditis* Genetics Center at the University of Minnesota. In addition, a FRET positive control strain designated *unc-54::CV* (with fused CFP and YFP coding sequences attached to an *unc-54* promoter) has been deposited there as strain DDP2.

## ACKNOWLEDGMENTS

Authors would like to thank Declan Brady for expert technical assistance; Benjamin Loader and Andrew Gregory (National Physical Laboratory, Teddington, United Kingdom) for SAR measurements (Fig. 1B); David Baillie and Bob Johnsen (Simon Fraser University, Burnaby, Vancouver, Canada) for providing strains BC20342 and BC20333; Aamir Nazir (CDRI, Lucknow, India) for sharing strain NL5901; Neil Telling (Medical School, University of Keele, United Kingdom) for loan of a Reflex sXc-1800 exposure system; and Manuel Murbach (Foundation for Research on Information Technologies in Society (IT<sup>2</sup>S), Zurich, Switzerland) for installing and calibrating this equipment on site at Nottingham. This work was supported by a summer bursary from the Nuffield Trust enabling participation by Nooria Iqbal.

## REFERENCES

- Abramson MJ, Benke GP, Dimitriadis C, Inyang IO, Sim MR, Wolfe RS, Croft RJ. 2009. Mobile telephone use is associated with changes in cognitive function in young adolescents. *Bioelectromagnetics* 30:678–686.
- Adey WR. 1993. Biological effects of electromagnetic fields. *J Cellular Biochem* 51:410–416.
- Ahuja YR, Sharma S, Bahadur B. 2013. Autism: An epigenomic side-effect of excessive exposure to electromagnetic fields. *Int J Med Med Sci* 5:171–177.
- Anbalagan C, Lafayette I, Antoniou-Kourouniotti M, Haque M, King J, Johnsen B, Baillie D, Gutierrez C, Rodriguez Martin J, de Pomerai D. 2012. Transgenic nematodes as biosensors for metal stress in soil pore water samples. *Exotoxicology* 21:439–455.
- Anbalagan C, Lafayette I, Antoniou-Kourouniotti M, Gutierrez C, Rodriguez Martin J, Chowdhuri DK, de Pomerai D. 2013. Use of transgenic GFP reporter strains of the nematode *Caenorhabditis elegans* to investigate the patterns of stress responses induced by pesticides and by organic extracts from agricultural soils. *Ecotoxicology* 22:72–85.
- Arendash GW, Mori T, Dorsey M, Gonzalez R, Tajiri N, Borlongan C. 2012. Electromagnetic treatment to old Alzheimer's mice reverses  $\beta$ -amyloid deposition, modifies cerebral blood flow, and provides selected cognitive benefit. *PLoS ONE* 7:e35751.
- Bodhicharla R, Nagarajan A, Winter J, Adenle A, Nazir A, Brady D, Vere K, Richens J, O'Shea P, Bell DR, de Pomerai D. 2012. Effects of  $\alpha$ -synuclein overexpression in transgenic *Caenorhabditis elegans*. *CNS Neurol Disord Drug Targets* 11:965–975.
- Carlberg M, Hardell L. 2012. On the association between glioma, wireless phones, heredity, and ionising radiation. *Pathophysiol* 19:243–252.
- Christopoulos C. 2006. The transmission-line modelling (TLM) method in electromagnetics. San Rafael, CA: Morgan & Claypool. pp 1–30.
- Consales C, Merla C, Marino C, Benassi B. 2012. Electromagnetic fields, oxidative stress, and neurodegeneration. *Int J Cell Biol* 2012:68397.
- Cotgreave IA. 2005. Biological stress responses to radio frequency electromagnetic radiation: Are mobile phones really so (heat) shocking? *Arch Biochem Biophys* 435:227–240.
- Croft RJ, Leung S, McKenzie RJ, Loughran SP, Iskra S, Hamblin DL, Cooper NR. 2010. Effects of 2G and 3G mobile phones on human alpha rhythms: Resting EEG in adolescents, young adults, and the elderly. *Bioelectromagnetics* 31:434–444.
- Daniells C, Duce I, Thomas D, Sewell P, Tattersall J, de Pomerai D. 1998. Transgenic nematodes as biomonitors of microwave-induced stress. *Mutat Res* 399:55–64.
- David DC, Ollikainen N, Trinidad JC, Cary MP, Burlingame AL, Kenyon C. 2010. Widespread protein aggregation as an inherent part of aging in *C. elegans*. *PLoS Biol* 8:e10000450.
- Dawe AS, Smith B, Thomas DWP, Greedy S, Vasic N, Gregory A, Loader B, de Pomerai DI. 2006. A small temperature rise may contribute towards the apparent induction by microwaves of heat-shock gene expression in the nematode *Caenorhabditis elegans*. *Bioelectromagnetics* 27:88–97.
- Dawe AS, Nylund R, Leszczynski D, Kuster N, Reader T, de Pomerai DI. 2008. Continuous wave and simulated GSM

- exposure at 1.8 W/kg and 1.8 GHz do not induce hsp 16–1 heat-shock gene expression in *Caenorhabditis elegans*. *Bioelectromagnetics* 29:92–99.
- Dawe A, Bodhicharla R, Graham N, May S, Reader T, Loader B, Gregory A, Swicord M, Bit-Babik G, de Pomerai D. 2009. Low-intensity microwave irradiation does not substantially alter gene expression in late larval and adult *Caenorhabditis elegans*. *Bioelectromagnetics* 30:602–612.
- Del Vecchio G, Giuliani A, Fernandez M, Mesirca P, Bersani F, Pinto R, Ardoino L, Lovisolo GA, Giardino L, Calza L. 2009. Effect of radiofrequency electromagnetic field exposure on in vitro models of neurodegenerative disease. *Bioelectromagnetics* 30:564–572.
- de Pomerai D, Daniells C, David H, Allan J, Duce I, Mutwakil M, Thomas D, Sewell P, Tattersall J, Jones D, Candido P. 2000. Microwave radiation induces a heat-shock response and enhances growth in the nematode *Caenorhabditis elegans*. *IEEE Trans Microw Theory Tech* 48:2076–2081.
- de Pomerai DI, Smith B, Dawe A, North K, Smith T, Archer DB, Duce IR, Jones D, Candido EPM. 2003. Microwave radiation can alter protein conformation without bulk heating. *FEBS Lett* 543:93–97.
- Deshmukh PS, Megha K, Banerjee BD, Ahmaed RS, Chandna S, Abegaonkar MP, Tripathi AK. 2013. Detection of low level microwave radiation induced deoxyribonucleic acid damage vis-à-vis genotoxicity in brain of Fischer rat. *Toxicol Int* 20:10–24.
- Gherardini L, Ciuti G, Tognarelli S, Cinti C. 2014. Searching for the perfect wave: The effects of radiofrequency electromagnetic fields on cells. *Int J Mol Sci* 15:5366–5387.
- Goedert M. 2015. Alzheimer's and Parkinson's diseases: The prion concept in relation to assembled A $\beta$ , tau, and  $\alpha$ -synuclein. *Science* 349:125555.
- Gordon GW, Berry G, Liang XH, Levine B, Herman B. 1998. Quantitative fluorescence resonance energy transfer measurements using fluorescence microscopy. *Biophys J* 74:2702–2713.
- Hardell L, Carlberg M, Soderqvist F, Hansson Mild K, Morgan LL. 2007. Long-term use of cellular phones and brain tumours: increased risk associated with use for  $\geq 10$  years. *Occup Environ Med* 64:626–632.
- Hardell L, Carlberg M, Hansson Mild K. 2013. Use of mobile phones and cordless phones is associated with increased risk for glioma and acoustic neuroma. *Pathophysiol* 20:85–110.
- INTERPHONE Study Group. 2010. Brain tumour risk in relation to mobile telephone use: Results of the INTERPHONE international case-control study. *Int J Epidemiol* 39:675–694.
- INTERPHONE Study Group. 2011. Acoustic neuroma risk in relation to mobile telephone use: Results of the INTERPHONE international case-control study. *Cancer Epidemiol* 35:454–464.
- Jiang DJ, Li J, Zhang J, Xu S, Kuang F, Lang H, Wang Y, An G, Li J, Guo G. 2013. Electromagnetic pulse exposure induces overexpression of beta amyloid protein in rats. *Arch Med Res* 44:178–184.
- Kaminski Schierle GS, Bertocini CW, Chan FTS, van der Goot AT, Schwedler S, Skepper J, Schlachter S, van Ham T, Esposito A, Kumita JR, Nollen EAA, Dobson CM, Kaminsky CF. 2011. A FRET sensor for non-invasive imaging of amyloid formation in vivo. *ChemPhysChem* 12:673–680.
- Kesari KK, Siddiqui MH, Meena R, Verma HN, Kumar S. 2013. Cell phone radiation exposure on brain and associated biological systems. *Indian J Exp Biol* 51:187–200.
- Leszczynski D, Joenvaara S, Reivinen J, Kuokka R. 2002. Non-thermal activation of the hsp27/p38MAPK stress pathway by mobile phone radiation in human endothelial cells: Molecular mechanism for cancer- and blood-brain barrier effects. *Differentiation* 70:120–129.
- Leszczynski D, de Pomerai D, Koczan D, Stol D, Franke H, Albar JP. 2012. Five years later: The current status of the use of proteomics and transcriptomics in EMF research. *Proteomics* 12:2493–2509.
- Liebl MP, Windschmitt J, Schafer A-K, Reber H, Behl C, Clement AM. 2015. Low-frequency magnetic fields do not aggravate disease in mouse models of Alzheimer's disease and amyotrophic lateral sclerosis. *Scientific Rep* 5:8585.
- Link C, Cypser J, Johnson C, Johnson T. 1999. Direct observation of stress response in *Caenorhabditis elegans* using a reporter transgene. *Cell Stress Chaperones* 4:235–242.
- Liu X, Zuo H, Wang D, Peng R, Song T, Wang S, Xu X, Gao Y, Li Y, Wang S, Wang L, Zhao L. 2015. Improvement of spatial memory disorder and hippocampal damage by exposure to electromagnetic fields in an Alzheimer's disease rat model. *PLoS ONE* 10:e0126963.
- Mattsson M, Simko M. 2012. Is there a relationship between extremely low frequency magnetic field exposure, inflammation and neurodegenerative diseases? A review of in vivo and in vitro experimental evidence. *Toxicol* 301:1–12.
- McCann H, Stevens CH, Cartwright H, Halliday GM. 2014.  $\alpha$ -Synucleinopathy phenotypes. *Parkinsonism Relat Disord* 20:S62–S67.
- Mitchell DH, Stiles JW, Santelli J, Sanadi DR. 1979. Synchronous growth and aging of *Caenorhabditis elegans* in the presence of fluorodeoxyuridine. *J Gerontol* 34:28–36.
- Mutwakil MHAZ, Steele TJG, Lowe KC, de Pomerai DI. 1997. Surfactant stimulation of growth in the nematode *Caenorhabditis elegans*. *Enz Microb Technol* 20:462–470.
- Nagarajan A, Bodhicharla R, Winter J, Anbalagan C, Morgan K, Searle MS, Nazir A, Adenle A, Fineberg A, Brady D, Vere K, Richens J, O'Shea P, Bell D, de Pomerai DI. 2015. A fluorescence resonance energy transfer assay for monitoring  $\alpha$ -synuclein aggregation in a *Caenorhabditis elegans* model for Parkinson's disease. *CNS Neurol Disord Drug Targets* 14:1054–1068.
- Nittby H, Grafstrom G, Tian DP, Malmgren L, Brun A, Persson BR, Salford LG, Eberhardt J. 2008. Cognitive impairment in rats after long-term exposure to GSM-900 mobile phone radiation. *Bioelectromagnetics* 29:219–232.
- Nittby H, Brun A, Eberhardt J, Malmgren L, Persson BR, Salford LG. 2009. Increased blood-brain barrier permeability in mammalian brain 7 days after exposure to the radiation from a GSM-900 mobile phone. *Pathophysiology* 16:103–112.
- Paul J, Christopoulos C, Thomas DWP. 1999. Generalised material models in TLM—Part 1: Materials with frequency-dependent properties. *IEEE Transact Antennas and Propagation* 47:1528–1534.
- Paul J, Christopoulos C, Thomas DWP. 2002. Simulation of general linear dielectric properties in TLM. *Int J Numer Model* 15:403–417.
- Perez-Castejon C, Perez-Bruzon RN, Llorente M, Pes N, Lacasa C, Figols T, Lahoz M, Maestu C, Vera-Gil A, del Moral A, Azanza MJ. 2009. Exposure to ELF-pulse modulated X

- band microwaves increases in vitro human astrocytoma cell proliferation. *Histol Histopathol* 24:1551–1561.
- R Core Team. 2014. R: A language and environment for statistical computing, R foundation for statistical computing, Vienna, Austria. URL <http://www.R-project.org/> [Last accessed 22 Nov 2015].
- Roberti MJ, Jovin TM, Jares-Erijman E. 2011. Confocal fluorescence anisotropy and FRAP imaging of  $\alpha$ -synuclein amyloid aggregates in living cells. *PLoS ONE* 6:e23338.
- Roodveldt C, Bertocini C, Andersson A, van der Goot A, Hsu S-T, Fernandez-Montesinos R, de Jong J, van Ham TJ, Nollen EA, Pozo D, Christodoulou J, Dobson CM. 2009. Chaperone proteostasis in Parkinson's disease: Stabilisation of the Hsp70/ $\alpha$ -synuclein complex by Hip. *EMBO J* 28:3758–3770.
- Sage C, Carpenter DO. 2009. Public health implications of wireless technologies. *Pathophysiology* 16:233–246.
- Schleofer B, Schlaefer K, Blettner M, Berg G, Bohler E, Hettinger I, Kunna-Grass K, Wahrendorf J, Schutz J. 2007. Environmental risk factors for sporadic acoustic neuroma (Interphone Study Group, Germany). *Eur J Cancer* 43:1741–1747.
- Schuderer J, Samaras T, Oesch W, Spät D, Kuster N. 2004. High peak SAR exposure unit with tight exposure and environmental control for in vitro experiments at 1800 MHz. *IEEE Transact Microwave Theor Tech* 52:2057–2066.
- Swain SC, Keusekotten K, Baumeister R, Sturzenbaum SR. 2004. *C. elegans* metallothioneins: New insights into the phenotypic effects of cadmium toxicosis. *J Molec Biol* 341:951–959.
- Tang J, Zhang Y, Yang L, Chen Q, Tan L, Zuo S, Feng H, Chen Z, Zhu G. 2015. Exposure to 900MHz electromagnetic fields activates the mcp-1/ERK pathway and causes blood-brain barrier damage and cognitive impairment in rats. *Brain Res* 1601:92–101.
- Terro F, Magnaudeix A, Crochetet M, Martin L, Bourthoumieu S, Wilson C, Yardin C, Leveque P. 2012. GSM-900MHz at low dose temperature-dependently downregulates  $\alpha$ -synuclein in cultured cerebral cells independently of chaperone-mediated autophagy. *Toxicology* 292:136–144.
- van Ham TJ, Thijssen KL, Breitling B, Hofstra RMW, Plasterk RHA, Nollen EA. 2008. *C. elegans* model identifies genetic modifiers of  $\alpha$ -synuclein inclusion formation during aging. *PLoS Genet* 4:e100027.
- van Ham TJ, Esposito A, Kumita JR, Hsu S-TD, Kaminski Schierle GS, Kaminski CF, Dobson CM, Nollen EAA, Bertocini CW. 2010. Towards multiparametric fluorescent imaging of amyloid formation: Studies of a YFP model of  $\alpha$ -synuclein aggregation. *J Molec Biol* 395:627–642.
- Williams P, Dusenbery D. 1990. Aquatic toxicity testing using the nematode, *Caenorhabditis elegans*. *Environ Toxicol Chem* 9:1285–1290.
- Wright JA, Brown DR. 2008. Alpha-synuclein and its role in metal binding: Relevance to Parkinson's disease. *J Neurosci Res* 86:496–503.
- Zuur AF, Ieno EN, Walker NJ, Saveliev AA, Smith GM. 2009. Mixed effects models and extensions in ecology with R. New York, NY: Springer Verlag. pp 101–142.